Supporting Information

Peddada *et al.* 10.1073/pnas.0808188105

SI Text

Results

Fibroid Growth Rate Determination. For each fibroid, the daily growth rate (or shrinkage rate) for a given time interval from one MRI scan to the next available MRI scan was estimated by dividing the change in (natural) log-volume during the interval by the number of days between MRI scans. Each interval between two MRI scans provided an estimate of the daily growth rate. Thus, for tumors with two or more MRI measurements, we had one, two, or three daily growth rates.

We conducted analyses to evaluate the validity of averaging the up to three available estimates of daily growth. Using mixed effects linear models, we found that the daily growth rate, averaged across all tumors across all women, did not differ significantly across time intervals ($P = 0.81$), nor did its variance. This indicates that there was no systematic effect associated with study time such as changes in MRI technology. Consequently, we improved the estimated average daily growth rate of each tumor by pooling the daily growth rate estimates from all available time points for that tumor. Hence, we averaged the estimated daily growth rates from all available time points for each tumor. However, we also analyzed the daily growth rates of a tumor based on each individual time interval, entering tumor and woman as random effects in the mixed model. The results so obtained mirrored the results of the analyses based on the average daily growth rates, although, as expected, they were subject to larger standard errors (data not shown).

Conversion of Daily Growth Rate to a 6-Month Percent Change in Volume. We converted the average daily growth rate (based on change in log-volume) of each tumor to a 6-month percent change in volume using the formula $100 \times (\exp(R) - 1)$. In this formula, R is the average growth rate (in natural log scale) indexed to 180 days (6 months). The logic behind the formula is as follows. For a given tumor, suppose that $\ln(V_1)$ and $\ln(V_2)$ are the log volumes at baseline and volume after 180 days of growth at the measured growth rate for the tumor. The 6-month growth rate of the tumor is then given by $\ln(V_2) - \ln(V_1) = \ln\left(\frac{V_2}{V_1}\right) = R$. The 6-month percent change in tumor volume of the same tumor is $100 \times \left(\frac{V_2}{V_1} - 1\right) = 100 \times (\exp(R) - 1)$, the formula above.

Rationale for Converting Growth Rates to a 6-Month Percent Change in Volume. There were two reasons for converting growth rates to a 6-month percent change. First, text books, such as *Comprehensive Gynecology* (1), suggest an initial clinical follow-up time of 6 months, indicating that this interval change would be an important clinical marker. Second, although the study protocol designated that tumor volume measurements be taken on each participant for up to four time periods spanning 1 year. Not every participant had four measurements for reasons that are detailed later (e.g., treatment). The median of the maximum length of time a participant was in the study was 265.5 days (slightly less than 9 months). Thus, converting growth rates to a 6-month percent change limited the possibility of extrapolation of the results.

Spontaneously Regressing Tumors. The data for the 19 spontaneously regressing tumors (>20% reduction in volume in 6 months) are provided in Table S1.

Factors Associated with Tumor Growth. For consistency and for clarity of clinical interpretation, we converted factors (e.g., age, tumor volume, BMI) that were measured on a continuous scale into categories. Age of the participant was separated into three categories based on standard age cuts to distribute the number of women among groups relatively equally, namely, younger than 35 years, at least 35 years of age but younger than 45 years, and 45 years or older. We categorized tumor volume into three categories based on the approximate diameter of the tumor by grouping those less than 3 cm (historical diameter limit set by Muram criteria) as a "small fibroid" group. We then divided the remaining tumors at a centimeter cut point that would maintain sufficient numbers in each of the upper categories. This resulted in a middle category of at least 3 cm but less than 5 cm and an upper category of 5 cm or more in diameter. The BMI was categorized into three standard categories for normal, overweight, and obese: less than 25, at least 25 but less than 30, and 30 or more. We categorized number of fibroids into four (1, 2, 3–8, and >8) to look at solitary tumors and those with only two tumors as separate groups, and then divided the remaining tumors into relatively equal groups. An advantage of converting continuous variables into categorical variables is that the results of the analysis do not depend on any unknown nonlinear relation that might exist between tumor growth and the continuous variables. Thus, categorical representation of various factors provides a more robust interpretation of the data.

Rationale for Model Selection. Initial examination of unadjusted mean growth rates by each category of the factors of interest revealed an effect of age that appeared to differ by ethnic group. Thus, our base model included an age-by-ethnicity term. A parsimonious "primary" model was built by adding additional variable(s) to this base model one by one. For each new resulting model, the Akaike information criterion was computed. We stopped including additional variables when doing so resulted in a substantial increase in the Akaike information criterion.

Linear Mixed Effects Model. We studied the effects of various factors on the average growth rate of each tumor by performing standard analysis of variance using linear mixed effects models. We treated the woman effect as the random effect and the remaining factors listed previously as fixed effects. Because multiple tumors were measured on all but five women, the correlation in mean growth rate between tumors within women was modeled using woman as a random effect, as commonly done in the analysis of repeated measures data. Such a model allowed us to estimate the variability in tumor growth rate between tumors within women (known as "within-woman variation") and to estimate the variability in the tumor growth rate between women (known as "between-women variation"). If the within-woman variability was extremely large, this implied that it was hard to predict the growth rate of a particular tumor by knowing the growth rate of a different tumor within the same woman. Similarly, if the between-woman variability was large, this implied that it was difficult to predict the average growth rate of tumors of a particular woman by knowing the average growth rates for a different woman.

Detection of Outliers. Because studentized residuals exceeding 3 are usually considered as potential outliers, the results of our analyses are based on dropping the 4 tumors that had studentized residuals exceeding 3. Thus, all our analyses of factors affecting growth rate were based on the remaining 258 tumors from 72 women. The primary estimates regarding age differences by ethnicity and tumor number do not change substantially when the four outliers are included, but the standard errors around those estimates tended to be larger. Interestingly, approximately 97% of the 262 tumors had studentized residuals within 2, consistent with a standard normal distribution. As one might expect, dropping the three additional outliers that had studentized residuals exceeding 2, we obtain stronger evidence of race-by-age interaction as well as the effect of number of tumors in the uterus. The statistical significance based on the 255 tumors was even more robust than the modeling with 258 tumors presented in the article.

Sensitivity/Robustness Analyses for Growth Rate Analyses. During the course of the study, the thickness of the MRI slices changed from greater than 5 mm ("thicker") slice technology to as small as 3 mm ("thinner") slice technology, which provided a more precise estimate of volume. To adjust for the change in slice thickness in each tumor image affected, we computed the average 6-month growth rate by weighting growth rate in each time interval by the reciprocal of the square root of average slice thickness between the two time points. Thus, growth rates based on the "thicker" slices were given smaller weight than the growth rates based on the "thinner" slices. The results of this weighted analysis mirrored those without weights. Hence, the results reported in the article are based on the unweighted analysis.

We also performed robustness studies to (*i*) directly compare subserosal with intramural tumors by excluding the six submucosal fibroids and (*ii*) verify that the small group of single tumors was not having undue influence by excluding them ($n = 5$). Results were essentially unchanged with these analyses, except, as expected, fibroid number was not important in the latter analysis.

Rapid Tumor Growth. Based on the frequency distribution of growth rate, the median growth rate was a modest 9%, but we note that as many as 40% of the tumors had an average increase in volume of greater than 20% per 6 months, indicating rapid growth. In this analysis, we were interested in studying the factors associated with tumors that displayed greater than 20% growth per 6 months. We called such tumors "rapidly growing tumors." We classified each tumor as to whether it was rapidly growing or not rapidly growing. Accordingly, the response variable of interest was "log-odds that a tumor was rapidly growing." As in the case of tumor growth analysis described earlier, we analyzed these repeated measures data by taking woman as a random effect, because multiple tumors were measured on most women. Because the response variable was log odds ratio, we used a mixed effects logistic regression model and the SAS macro "GLIMMIX" (SAS Institute, Cary, NC) to conduct these analyses. Results are summarized in Table S2. The odds of growing rapidly were significantly associated with age, and the association differed by ethnicity ($P = 0.002$ for the age-by-ethnicity interaction). The direction of associations generally mirrored results for the analysis of continuous growth. The relative odds of rapid growth declined dramatically with age for whites ($P < 0.001$), but there was little difference by age for blacks ($P = 0.81$).

SI Discussion

Age and Race of Women Sampled: Consideration of Potential Bias. A major conclusion of our study is that black and white women had different patterns of fibroid growth depending on their age. Fibroid growth rate was rapid for tumors from both young black and young white women (<35 years of age) and declined with increasing age for whites but not for blacks ($P = 0.05$). We considered whether this result was an artifact of the ages of women recruited in the study. Although possible, we believe there is sufficient evidence in our data to conclude that these results were not attributable to such a length-biased sampling.

Our conclusions would be wrong in the following two instances: (*i*) systematically, the young blacks had a myomectomy before entering the study removing the fast-growing tumors, and (*ii*) systematically, the older whites had a myomectomy before entering the study removing the fast-growing tumors. In our data, neither of these two possibilities was seen. Only four patients had fibroid-related surgery before entering the study. Of these four, only one young black woman (32 years old) had a myomectomy, which was nearly 2 years before enrollment in the study. Two black women and one white woman from the middle age group (between 35 and 45 years) had a myomectomy more than 2 years before enrolling in the study.

Variation in Menstrual Phase: Consideration of Potential Bias. Women were interviewed monthly and asked about menses. The 12 days before start of menses were designated as the "luteal phase." Fibroid tissue has been reported to show more evidence of proliferation during the luteal phase, so we categorized MRI dates by luteal phase or nonluteal phase. We did not have this information on 2 of the 72 women, and 20 of the women were excluded for use of oral contraceptive or hormonal medication. To evaluate if fibroid growth might be influenced by women's menstrual cycle phases, we investigated if there were any phase differences among the women in our study by race and age. Specifically, we were concerned if older white women belonged systematically more often to one of the phases and if older black women belonged systematically to a different phase. For each woman, we computed the difference between the number of times she was in the non-luteal phase and the number of times she was in the luteal phase. We found that the mean of this difference did not differ significantly among the six age-by-race groups ($P = 0.7$).

Hormonal Use and Time of Initial Fibroid Diagnosis: Consideration of Potential Bias. We compared women of different races and age groups in terms of hormone use to make sure that our tumor growth results were not attributable to differences in the use of hormones by blacks and whites. Of the 72 participants, we found that 20 used some form of hormonal medication, the majority of whom used oral contraceptives, and that 52 did not. We did not find any significant difference among the six age-by-race categories ($P = 0.50$). However, as expected, we did see a significant age effect, with younger women using hormones significantly more than older women ($P = 0.02$). This result does not explain the tumor growth reported in the article. A similar analysis of time of initial fibroid diagnosis showed no evidence that this selection factor could have biased results.

SI Methods

MRI Protocol. Of the 72 women in the growth analysis, 17 completed two MRI scans, 16 completed three MRI scans, and 39 completed four MRI scans. Reasons for completing less than four MRI scans were treatment (7 after two MRI scans and 3 after three MRI scans), study ending (10 after two MRI scans and 9 after three MRI scans), and dropping out (4, all after three MRI scans).

A standard fibroid protocol was performed on all participants using a 1.5-T MRI scanner (Siemens Avanto, Malvern, PA) with the phased-array surface coil. The protocol consisted of the following sequences and parameters: T2-weighted, half-Fourier, single-shot turbo spin-echo (repetition time [TR]/echo time [TE]/Flip Angle [FA]: 1,500 msec/90 msec/180) in both the axial

and sagittal planes; T2-weighted turbo spin echo images in both the axial (TR/TE/FA: 3,640 msec/96 msec/180) and sagittal (TR/TE/FA: 5,750 msec/98 msec/180) planes; precontrast non-fat-suppressed, T1-weighted, two-dimensional (2D), spoiled gradient echo [SGE (TR/TE/FA: 142 msec/4.4 msec/70)] in the axial plane; precontrast fat-suppressed, T1-weighted, 2D, SGE (TR/TE/FA; 233 msec/4.76 msec/70) in the axial plane; postcontrast T1-weighted, 2D, SGE (TR/TE/FA; 137 msec/4.4 msec/70) in the sagittal plane; postcontrast three-dimensional, SGE, Volume Interpolated Breath-hold gradient Echo [VIBE] (TR/TE/FA: 4.87 msec/2.36 msec/10) in the sagittal plane; and fat-suppressed, 2D, SGE (TR/TE/FA: 233 msec/4.76 msec/10) in the axial plane. Postcontrast T1-weighted images were acquired after i.v. bolus injection of 0.1 mmol/kg gadolinium chelate (Omniscan; Amersham Health, New York, NY) at 2 ml/sec using a power injector.

At the beginning of the study, the images across the pelvis were at least 7 mm apart (slice thickness plus gap). Because technology was upgraded at the MRI center, this was reduced to less than 5 mm apart midway through the study. Of the 825 tumor volume measurements, 71% were based on slice thickness ≤5 mm.

Measurement of Fibroids and Quality Assurance. Fibroids seen in sagittal T2-weighted images (Fig. S1) were measured using the manual outlining option in the volume estimation and tracking over time (VETOT) method. Volume determinations were made by two trained technicians. For a given tumor, the same technician measured the volume at all time points so that the change in volume over time was not confounded by any differences between the two technicians. To assess reliability of measurements, two technicians repeated measurements of both a large tumor and a small tumor in four MRI scans. The estimated intratechnician coefficient of variation was less than 1%, and growth rates of the two tumors showed no significant difference between the two technicians ($P = 0.57$).

To ensure the accuracy of the volume data obtained from MRI, we performed several quality assurance tasks. Because each woman had several fibroids measured over time, one possible source of error was misalignment of a given tumor over time. Once all volumetric measurements were obtained, each woman's MRI scans were reviewed to make sure the tumors were matched correctly across all time points.

As the technician traces each section of a tumor obtained from an MRI, the VETOT software computes the volume of that section. For example, Fig. S2 represents the volume of each MRI slice of a tumor. For this particular tumor, there were 17 slices numbered from image 3 to image 19 (x axis), and at each slice, the corresponding point on the y axis was the volume of the slice (in cubic millimeters) as determined by VETOT.

Thus, in an idealized situation, the shape of the curve would be "parabolic" with the two ends of the parabola close to "zero" (but never 0 because of the thickness of the MRI slices). The lack of smoothness to the parabola was attributable to variation in shape of the tumor and noise in the images. Because the two ends of the parabola in Fig. S2 were less than 1,000 mm^3, we believed that the tumor volume in this case was reasonably complete. Volumes of tumors with plots resembling Fig. S2 were considered reliable for the growth analysis.

In some MRI scans, a portion of the tumor (especially in extremely large tumors) was outside the view of the MRI scan or the image of one of the ends of the tumor had unclear boundaries for the technician to trace. In such cases, one of the ends of the parabola appeared to "hang" well above the horizontal axis, as seen in Fig. S3, which has five slices going from image 11 to image 15. Tumors with plots resembling Fig. S3 required further scrutiny. If a technician missed a recognizable portion at the end of the tumor, which might happen when the tumor boundary was indistinguishable from the uterine boundary, the extra portion was measured (usually 1 additional slice) and the volume of the tumor was recalculated. Eleven percent (89 of 824) of the volume measurements had a missed portion added in the quality control phase. These additional measurements were done primarily by a single technician. If a large tumor extended beyond the lateral position of the femur such that fibroid volume was not completely captured, its tumor volume was dropped from the analysis of that time point. When two tumors were recorded as one because of adjacent edges that were difficult to discriminate, we dropped these from analysis or used the volumes of the separate tumors only in the MRI visits for which the boundary could be assessed.

A third source of error in volume measurements was overlap of images. In some instances, the MRI operator had to stop scanning and then restart again. The resultant two files were manually combined to ensure that there was no duplication of slices or loss of slices in computing the tumor volume.

Conversion of Volume to Diameter of Fibroid. Although all statistical analyses were performed using the volume of tumor calculated from MRI scans, for the reader's ease of interpretation, in addition to the actual tumor volume, we also provided an approximate diameter using the standard ellipsoidal formula. In the formula, we assumed that all three diameters of the ellipsoid are of equal length. Thus, an approximate diameter of a fibroid is given by the formula $\text{diameter} = (0.52 * \text{volume})^{1/3}$.

Measurement of Uterine Volume. The uterine length was measured from the fundus to the external cervical os in the midline sagittal view, and the anterior/posterior diameter was measured at the widest point perpendicular to length in the same image. Width was measured in the axial view at its greatest dimension. Each MRI scan was inspected to ensure that any subserosal fibroid that was included in the diameter measure for the first MRI scan because it expanded the uterine boundaries was also included at the last MRI scan.

Fibroid Location. Location of fibroids within the uterus was based on the illustration (Fig. S4) defining the borders of the fundus, corpus, lower uterine segment, and cervical anatomical regions of the uterus.

1. Katz V, Lentz G, Lobo R, Gershenson D, eds (2007) *Comprehensive Gynecology* (Mosby, St. Louis), 5th Ed.

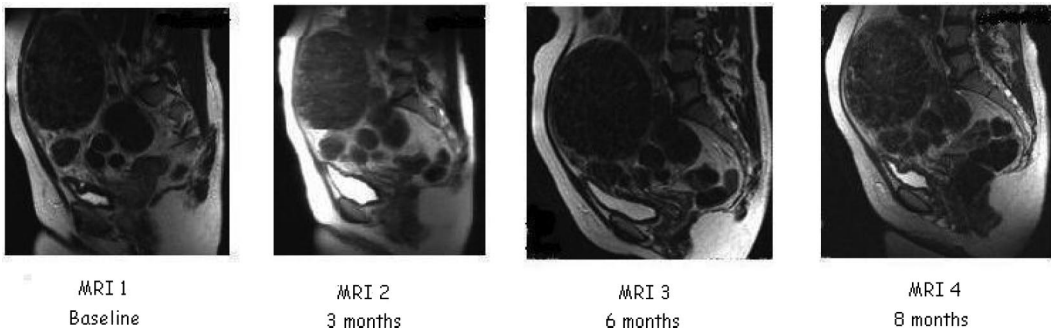

Fig. S1. Abdominal MRI scan of a study participant taken at four time points.

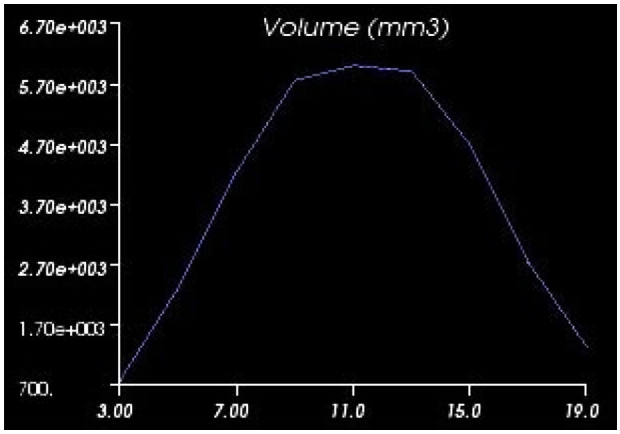

Fig. S2. Tumor completely measured. Volume of each MRI slice of a tumor (*y* axis) against the slice number (*x* axis).

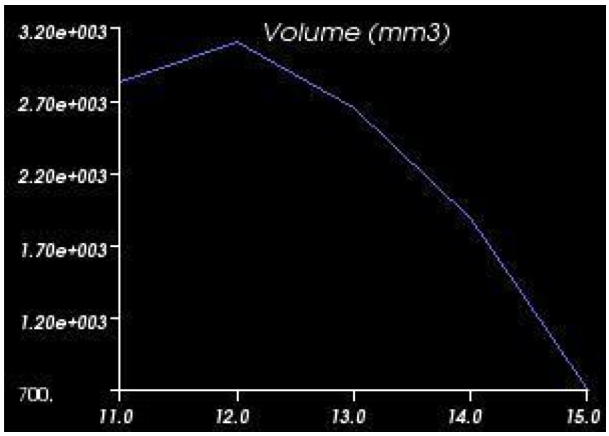

Fig. S3. Tumor incompletely measured. Volume of each MRI slice of a tumor (*y* axis) against the slice number (*x* axis).

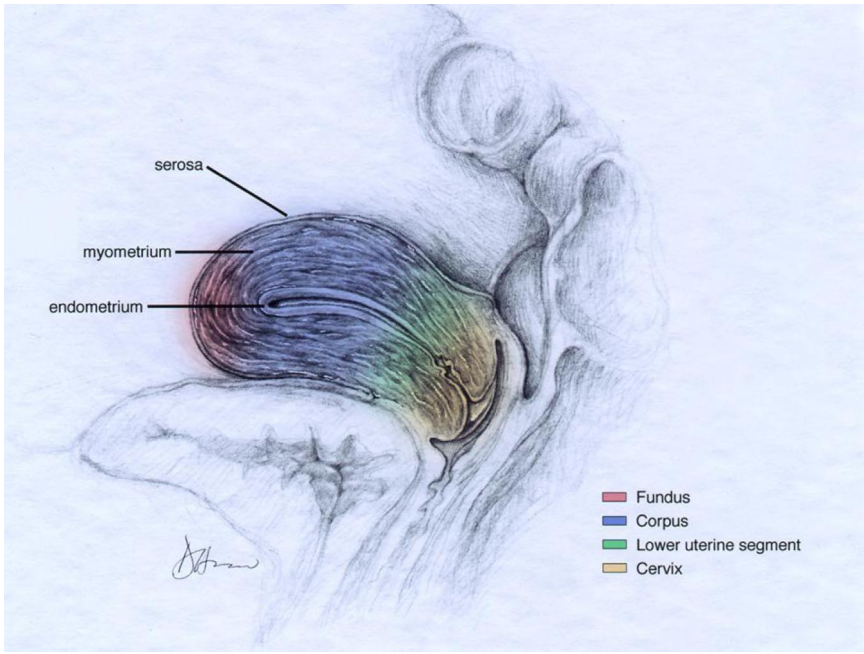

Fig. S4. Anatomical regions of the uterus. (Artwork by Dr. Diane Armao).

Table S1. Fibroids with greater than 20% reduction in volume per 6 months (N = 19 tumors from 14 women ordered by growth rate)

Subject ID	Race	Age	Initial Volume (cm^3)	Fibroid type	Fibroid location	Growth rate (%)	Estimated necrosis (%)
n	Black	40.4	39.30	Intramural	Corpus	−88.5	100
m	Black	37.6	12.65	Subserosal	Corpus	−68.7	100
c	Black	34.1	43.64	Intramural	Lower segment	−65.1	20
n	Black	40.4	10.43	Subserosal	Fundus	−61.3	75
e	Black	31.8	5.24	Subserosal	Corpus	−46.0	0
i	Black	42.4	21.63	Subserosal	Corpus	−44.1	80
d	White	46.3	7.82	Intramural	Fundus	−41.9	0
g	Black	44.9	16.96	Intramural	Fundus	−41.5	0
f	Black	30.1	5.05	Intramural	Fundus	−35.8	80
a	Black	45.6	33.20	Intramural	Lower segment	−34.5	90
b	White	46.5	16.59	Subserosal	Corpus	−33.2	0
m	Black	37.6	26.45	Subserosal	Lower segment	−28.9	40
k	Black	37.9	5.58	Intramural	Fundus	−27.0	5
l	White	32.9	21.63	Subserosal	Fundus	−24.8	0
h	Black	48.5	3.69	Intramural	Lower segment	−23.4	0
f	Black	30.1	23.91	Intramural	Corpus	−23.2	55
b	White	46.5	63.15	Subserosal	Lower segment	−21.0	0
j	Black	38.5	20.49	Intramural	Corpus	−20.5	0
j	Black	38.5	36.92	Intramural	Lower segment	−20.1	0

ID, identification.

Table S2. Adjusted* relative odds of at least a 20% growth rate per 6 months associated with factors of interest

Factor	*P* value†	Adjusted odds ratio (95% confidence interval)
Age by ethnicity, yr	0.002	
Blacks <35		Reference
Blacks 35–44		0.61 (0.23, 1.60)
Blacks ≥45		1.17‡ (0.33, 4.07)
Whites <35		Reference
Whites 35–44		0.35 (0.10, 1.30)
Whites ≥45		0.06§ (0.02, 0.25)
Number of fibroids	0.14	
>8		Reference
3–8		2.01 (0.98, 4.15)
2		0.57 (0.13, 2.50)
1		3.06 (0.29, 32.33)
BMI	0.38	
<25		Reference
25–29.9		0.55 (0.23, 1.33)
≥30		0.64 (0.27, 1.55)
Parity	0.13	
0		Reference
1		0.50 (0.20, 1.23)
Initial fibroid volume (diameter¶)	0.14	
<14.0 cm^3 (<3 cm)		Reference
14.0 cm^3–64.9 cm^3 (3.0–4.9 cm)		0.56 (0.28, 1.10)
≥65 cm^3 (5.0 cm)		0.53 (0.24, 1.18)
Type‖	0.60	
Intramural		Reference
Subserosal		1.17 (0.64, 2.14)
Location	0.44	
Corpus		Reference
Fundus		0.62 (0.30, 1.30)
Lower segment		0.95 (0.46, 1.94)

Here, $n = 258$ fibroids from 72 women. Four statistical outliers (all shrinking >50% in volume per 6 months) were excluded, leaving 258 fibroids.

*Age by ethnicity differences are adjusted for number of fibroids; number of fibroid differences are adjusted for age by ethnicity; all other variables are adjusted for age by ethnicity and number of fibroids.

†*P* value for the overall importance of each factor.

‡Pair-wise odds ratio is not statistically significant ($P = 0.81$).

§Pair-wise odds-ratio is statistically significant at $P < 0.001$.

¶Diameter calculated from measured volume based on ellipsoid formula.

‖Intramural includes six submucosal fibroids.